PCCP

PAPER

View Article Online
View Journal | View Issue

Cite this: *Phys. Chem. Chem. Phys.*, 2016, **18**, 28033

Wetting behavior of water on silicon carbide polar surfaces

W. W. Zhong,†[ab] Y. F. Huang,†[a] D. Gan,[a] J. Y. Xu,[a] H. Li,[a] G. Wang,[a] S. Meng*[ac] and X. L. Chen*[ac]

Received 6th July 2016,
Accepted 13th September 2016

DOI: 10.1039/c6cp04686j

www.rsc.org/pccp

Technically important wide band-gap semiconductors such as GaN, AlN, ZnO and SiC are crystallized in polar structures. Taking SiC as an example, we investigate the effect of surface polarity on the wetting behavior by water using experiments and molecular dynamic simulations. It is found that the contact angle (CA) of deionized water on the carbon-face (C-face) is significantly larger than that on the silicon-face (Si-face) for both 6H-SiC and 4H-SiC, while the CA of tetrachloromethane is almost the same on these two faces. This finding clearly indicates that polar interactions between water and SiC induce such a large difference in the CA. Extensive molecular dynamics simulations suggest that a larger CA on the C-face than that on the Si-face is resulted from the different charge agglomeration on the two faces. These results will not only be helpful in improving the state of the art processes such as rinsing and wet etching in device fabrication, but also offer a reliable method to determine the polarity of SiC crystals quickly, simply, accurately and nondestructively, which is easily extendable for the measurement of other polar crystals.

Introduction

Wetting is a ubiquitous phenomenon in daily life and industrial processes. It is characterized by the contact angle that reflects the ability for a liquid to spread out on a solid surface. Many technological processes for fabricating a semiconductor device such as etching and rinsing are required to control the wetting behavior. The wetting behaviors of liquids on a variety of solid surfaces have been well studied and understood over the last few decades.[1–4] Recent progress in wetting of water on several newly-developed materials indicates that wetting is very sensitive to surface structures. Using molecular dynamics simulations, Giovambattista *et al.*[5] observed that the CA decreases as the surface polarity increases. Wang *et al.*[6] showed that the hexagonal surface structure with a large dipole moment would induce a hydrophobic water monolayer, resulting from extremely strong electrostatic interactions between the substrate and water. James *et al.*[7] presented experimental evidence for the hydrophobic water layer near the surface of self-assembled monolayers. Shih *et al.*[8] reported that the CA of water decreases from 135° to 95° on graphene-treated glass with silica nanoparticles. Little, however, is known about the effect of polarity on wetting.

The wide band-gap semiconductor silicon carbide (SiC) has found applications in the new generation of electronic devices that have advantages such as energy saving, environmental friendliness, low weight, high power output *etc.* due to its high critical electric field, thermal conductivity, saturation carrier velocity and chemical stability.[9–12] Like other wide band-gap semiconductors such as GaN, AlN and ZnO, 6H- and 4H-SiC also crystallize in polar space group $P6_3mc$, their Si–C atomic dimers stack along the [0001] direction by ABCACB and ABCB, respectively. The schematic diagrams of the crystal structure are shown in Fig. 1. They both have two polar faces, *i.e.* the C-terminated polar face (C-face, $[000\bar{1}]$) and the Si-terminated polar face (Si-face, 0001). The existence of polarity is due to the difference in electronegativity of Si and C, and one of the four

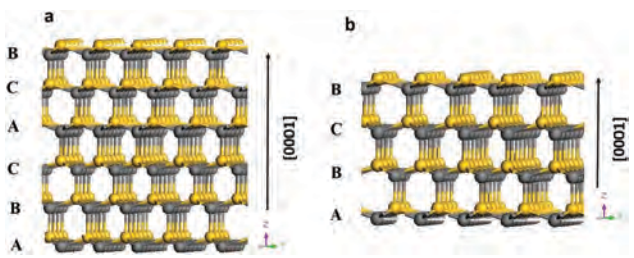

Fig. 1 Schematic diagrams of the crystal structure for (a) 6H-SiC and (b) 4H-SiC, the gold and gray balls represent Si and C atom, respectively.

[a] *Beijing National Laboratory for Condensed Matter Physics, Institute of Physics, Chinese Academy of Sciences, Beijing 100190, China. E-mail: xlchen@iphy.ac.cn, smeng@iphy.ac.cn*
[b] *Department of Materials, Taizhou University, Taizhou 318000, China*
[c] *Collaborative Innovation Center of Quantum Matter, Beijing, China*
† W. W. Zhong and Y. F. Huang contributed equally.

Si–C bonds is slightly longer than the other three. The two polar faces have strikingly different influences on the physical and chemical properties of the material even under an identical condition.[13–17] Fernandez-Garrido *et al.*[18] studied the effect of SiC surface polarity on the spontaneous formation of GaN nanowires and found that the surface polarity, nucleation, distribution and morphology of GaN are closely dependent on the polarity of SiC substrates. Kusunoki *et al.*[19] showed that carbon nanotubes formed on the C-face of SiC while graphite formed on the Si-face, even though SiC was treated under the same condition. Moreover, He *et al.*[20] found that the Si-terminated interface is more adhesive while less relaxative than the C-terminated interface through studying the Si(111)/6H-SiC(0001) heterojunction interface.

Here, by studying the wetting properties of deionized water on SiC polar crystals, we find that the water contact angle (CA) on the C-face of SiC is significantly larger than that on the Si-face for both 6H- and 4H-SiC. The carrier density, however, has little effect, if any, on the wetting behaviors. Extensive molecular dynamics simulations have revealed that the CA difference is resulted from the electrostatic interactions between water and substrates, which depend on charge transfer between C and Si atoms on different SiC faces. With these findings we propose a new method to distinguish polar faces by making use of water wetting on polar substrates, which is quick, convenient, intuitive and nondestructive. More importantly, they will be helpful in improving the rinsing and wet etching processes in fabricating SiC based electronic devices. We also elucidate the atomistic mechanism of observed wetting behaviors of water on the SiC surface.

Experiments and simulations

2-inch 6H-SiC and 4H-SiC wafers (TankeBlue, Beijing) were used for the CA measurements. Before measurements, the wafers were first degreased with acetone and methanol, rinsed with deionized water, and blown dry with nitrogen gas. Then the SiC wafers were packaged by nitrogen. The micro-morphology and surface roughness were determined using an atomic force microscope (AFM, Benyuan CSPM 400). Raman scattering experiments were performed using a high-resolution Raman spectrometer HR800 (Horiba JobinYvon) with a 532 nm laser excitation. CA measurements were performed on an OCA20 (Dataphysics, German), deionized water was employed as a probe liquid and each CA in figures is the average value of five measurements at five different positions in the same sample. The CA was measured by taking picture on a microscope. All measurements were carried out in ambient atmosphere at room temperature.

For molecular dynamics simulations, atomistic slab models with perfect C-/Si-faces are used to simulate the wetting behavior of water on SiC surfaces. Simulation is carried out on a substrate of 10.500×10.392 nm^2. Both 6H-SiC and 4H-SiC contain 6 silicon–carbon double atomic layers. A cubic box of water molecules with a size of $3 \times 3 \times 3$ nm^3 is initially put at a position of 5 Å above the substrate. Periodic boundary conditions are applied in x, y and z directions and the simulation box size is $10.500 \times 10.392 \times 10$ nm^3. The simulation is performed in the *NVT* ensemble at 300 K with the SPC/E water model.[21] Electrostatic interaction is considered by particle-mesh Ewald[22] with a real-space cutoff of 10 Å, and the cutoff for van der Waals interactions is also 10 Å. Lennard-Jones parameters for silicon and carbon atoms are σ_{Si-Si} = 0.34 nm, ε_{Si-Si} = 0.5336 kJ mol^{-1} and σ_{C-C} = 0.3426 nm, ε_{C-C} = 0.40 kJ mol^{-1}, respectively. The final 600 ps data of the whole 6 ns are collected for CA estimations. All the calculations are performed by using the Gromacs package.[23] Based on the previous report[24] that charge transfer in SiC was from the Si-atom to the C-atom with an electron transfer amount over 2e, it is thus reasonable to endow Si atoms with charges of +2.00e, +2.25e and +2.50e, and C atoms with a charge −2.00e, −2.25e and −2.50e, respectively.

Results and discussion

The surface roughness may have a notable influence on the measured contact angle values. In order to analyze the surface roughness of the samples, we first adopted AFM to study all the 6H- and 4H-SiC samples. From Fig. 2 and Table 1, it can be clearly seen that both the Si-face and the C-face of 6H- and 4H-SiC samples are smooth, with an average roughness less than 0.6 nm. Besides, it could be found that the Si-faces are generally smoother than the C-faces for all samples, which may be determined by the surface characteristics of the carbon polar face. Conducting (Cond) and semi-insulating (Semi) SiC are obtained by nitrogen- and vanadium-doping,[25–27] respectively. The effect of doping is neglected in the simulation since the doping concentration is low (doping concentration: 0.01 at% for N, 0.004 at% for V).

SiC has many different polytypes, which differ in the stacking sequence of the silicon–carbon double atomic layer along the c axis. Among them, 6H- and 4H-SiC are the most commonly used in devices, we choose these two polytypes for wetting measurements in our investigation. The polytype of SiC is confirmed using Raman spectroscopy as discussed in a previous report.[28] Raman spectra of 6H- and 4H-SiC are shown in Fig. 3. It could be seen that folded transverse acoustic (FTA) doublet mode of 4H-SiC owns a higher wavenumber compared with those of 6H-SiC, whereas 6H-SiC possesses a smaller FTO peak at ~750 cm^{-1} consistent with the previous reports.[29–31]

CAs on different SiC samples are shown in Fig. 4, where Fig. 4a and b are side-views of a water droplet on SiC surfaces. From these figures, we notice that wetting on the C-face and the Si-face is strikingly different. For both 6H- and 4H-SiC, CA values on the C-face are larger than that on the Si-face. In Fig. 4c, for conductive 6H-SiC (6H Cond), the CA is 34° on the C-face and 11° on the Si-face; and for semi-insulating 6H-SiC (6H Semi), the CA is 52° on the C-face and 36° on the Si-face. The wetting differences are 23° and 16° for 6H Cond and 6H Semi, respectively. This observation manifests that CAs of water on the C-face and the Si-face are quite different, where the CA on the C-face is always larger than that on the Si-face.

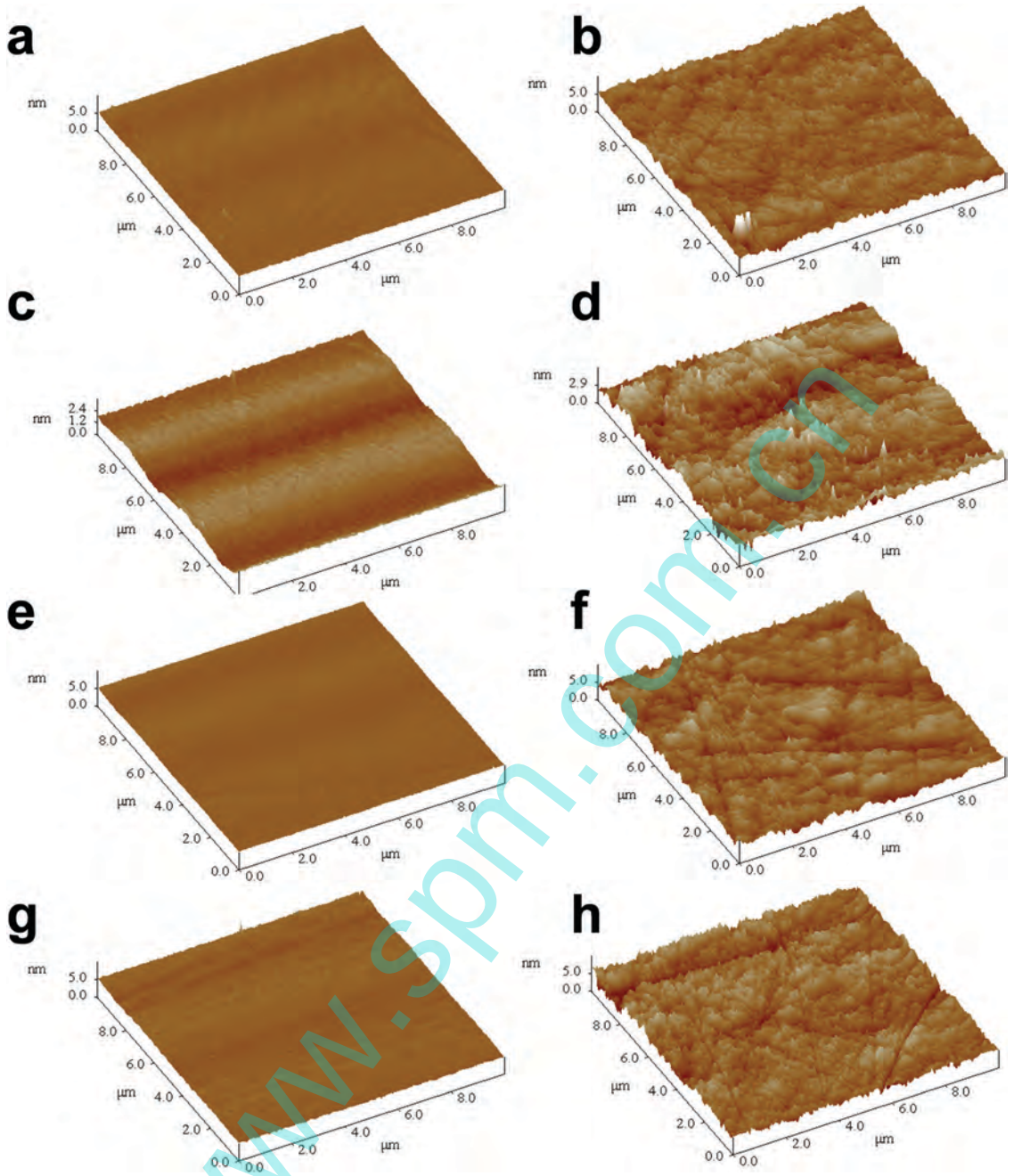

Fig. 2 AFM images of the surfaces for the (a) Si-face of 6H-SiC Semi, (b) the C-face of 6H-SiC Semi, (c) the Si-face of 6H-SiC Cond, (d) the C-face of 6H-SiC Cond, (e) the Si-face of 4H-SiC Semi, (f) the C-face of 4H-SiC Semi, (g) the Si-face of 4H-SiC Cond, (h) the C-face of 4H-SiC Cond.

Table 1 The surface roughness of various SiC faces

Samples	C-face (nm)	Si-face (nm)
6H Semi	0.459	0.103
6H Cond	0.428	0.061
4H Semi	0.577	0.101
4H Cond	0.628	0.149

Using the same method, we measure wetting of water on 4H-SiC as shown in Fig. 4d. CAs on the C-face and the Si-face of 4H Cond are 53° and 47°, and CAs on the C-face and the Si-face of 4H Semi are 50° and 46°. Wetting differences are 6° and 4°, respectively. The CA on the C-face is also larger than that on the Si-face.

In order to further study the phenomenon, we also use nonpolar tetrachloromethane as a probe liquid besides the polar water. Results are shown in Fig. 5. For 6H-SiC, the CA on the C-face is 6°, on the Si-face 8° and for 4H-SiC, the CA on the C-face is 5°, on the Si-face 6°. There is almost no CA difference of tetrachloromethane on the C-face and the Si-face if the uncertainty and error bars during the measurements are taken into consideration. Based on the CA values, we refer

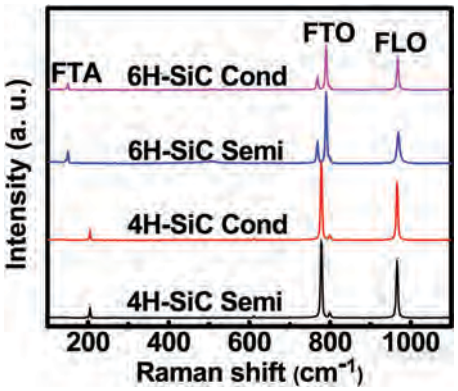

Fig. 3 Raman spectra of 6H- and 4H-SiC.

that electrostatic interactions between the polar probe liquid (such as water) and the surface cause wetting difference on SiC, whereas surface roughness of the samples is not a major factor. Both 4H- and 6H-SiC crystallize in a polar space group $P6_3mc$. The Si-terminated surface is positively charged, and the C-terminated surface is negatively charged. When contacting with H_2O molecules, two kinds of surface do make difference in polarizing them, resulting in a stronger electrostatic interaction on the Si-terminated surface than on the C-terminated surface. For details, see the MD simulation in the present manuscript. As for the atomic surface structure, both 4H- and 6H-SiC exhibit a stepped structure with the terrace (0001) or (000$\bar{1}$) for minimizing the surface energy.

We employed molecular dynamics simulations to investigate the molecular origin of the wetting difference on SiC. We calculated CAs on different polar faces and then analyzed the water molecule distribution near the surface. According to the *ab initio* calculations,[24] the charge transfer in SiC from the Si atom to the C atom can vary in a large range in different environments with no precise value. Therefore, in order to give a comprehensive description, we consider three conditions related to typical charge transfer amounts in our simulations. We assume three cases for charge transfer from the Si to C atom: +2 electrons (2.00*e*), +2.25 electrons (2.25*e*) and +2.50 electrons (2.50*e*). Consequently, C atoms possess a charge of −2.00*e*, −2.25*e* and −2.50*e*.

Water wetting angles on 6H-SiC and 4H-SiC are calculated without considering the effect of ultralow doping. In Fig. 6a, it could be seen that for 6H-SiC, the CA on the C-face decreases from 96° in the condition of C/Si atoms containing −2.00/+2.00*e* to 48° in C/Si atoms containing −2.50/+2.50*e*. The CA on the Si-face is 40° and 18° for these two charges, respectively. For 4H-SiC in Fig. 6b, the CA on the C-face is 80° for C/Si atoms containing −2.00/+2.00*e* and becomes 47° for C/Si atoms containing −2.50/+2.50*e*. On the Si-face, the two homologous CA values are 72° and 43° respectively. This fact shows that more charges transferred from Si to C cause a smaller CA, since more charges would induce a larger electron interaction.

We further analyze the water density along the direction perpendicular to SiC substrates. In Fig. 6c, the density as a function of height of the droplet starting from the SiC surface is plotted and the case of C/Si atoms containing −2.00/+2.00*e* is taken as example. It could be found for 6H-SiC first that the density peak of water droplet is 1.94 g cm^{-3} on the C-face and 1.93 g cm^{-3} on the Si-face. However, the positions of the two peaks are 0.287 nm (Si-face) and 0.387 nm (C-face) respectively. This first peak is caused by the interaction between atoms in

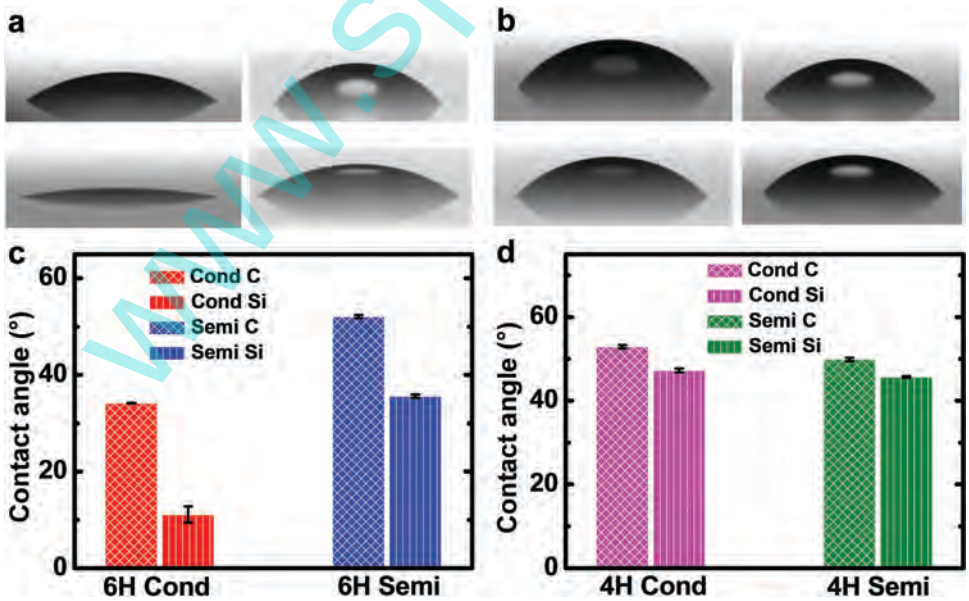

Fig. 4 Wetting of deionized water on 6H-SiC and 4H-SiC. (a) Side-view of the water droplet profile on the C/Si-face of conductive 6H-SiC (left two panels) and semi-insulating 6H-SiC (right two panels). (b) Side-view of the water droplet profile on the C/Si-face of conductive 4H-SiC (left two panels) and semi-insulating 4H-SiC (right two panels). (c) CA of water droplets on 6H-SiC. For conductive 6H-SiC, CAs on the C-face and the Si-face are 34.1° and 11.1° respectively. For semi-insulating 6H-SiC, the CA on the C-face is 52.1° and on the Si-face is 35.6°. (d) For 4H-SiC, CAs on the C/Si-face are 52.9°/47.2° (4H Cond), 49.8°/45.7° (4H Semi-insulating), respectively.

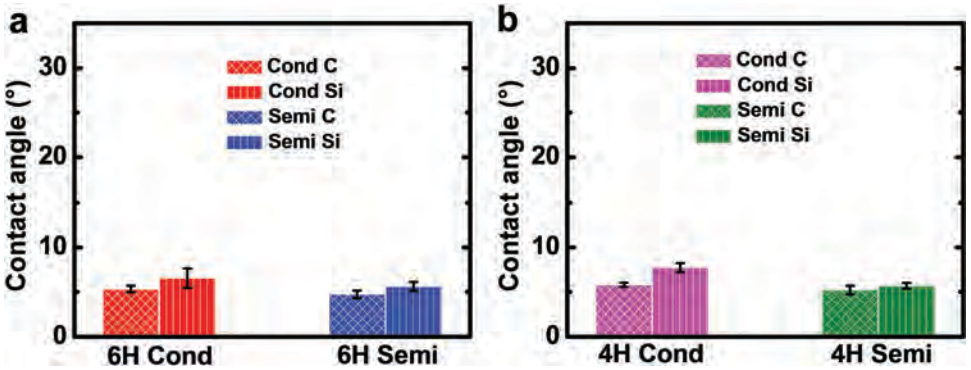

Fig. 5 Wetting of tetrachloroethane (CCl_4) on 6H-SiC and 4H-SiC. (a) For 6H-SiC, CAs on C-/Si-face are 5.3°/6.6° (Cond) and 4.7°/5.6° (Semi-insulating), respectively. (b) For 4H-SiC, CAs on the C-/Si-face are 5.8°/7.7° (Cond) and 5.2°/5.7° (Semi-insulating) respectively. The results indicate that there is almost no difference between nonpolar van der Waals interactions on the C-face and on the Si-face.

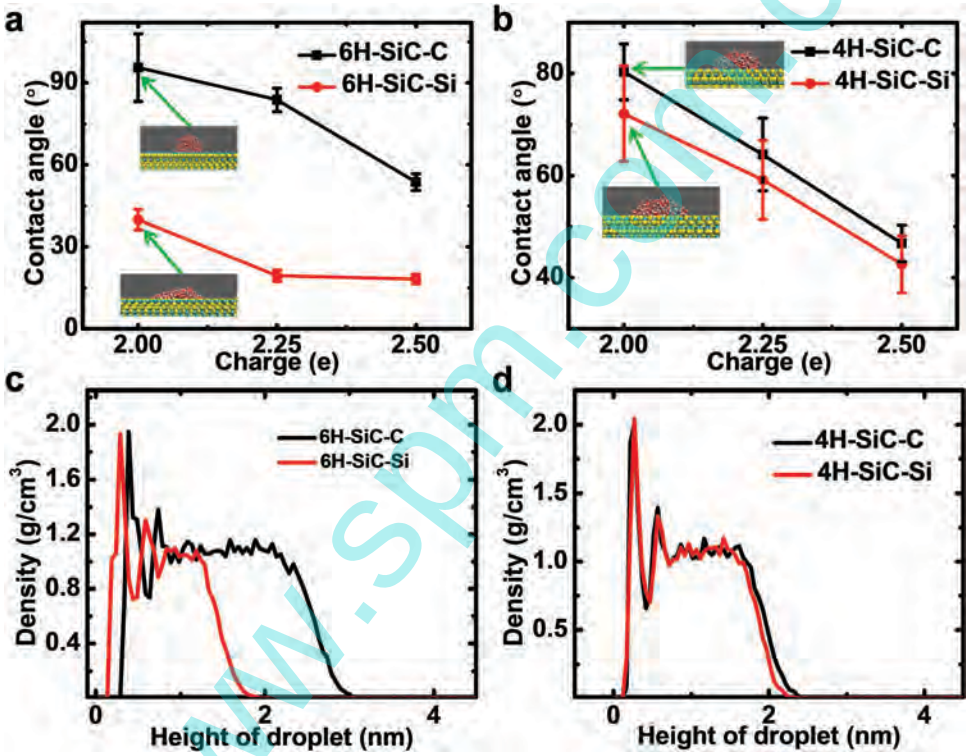

Fig. 6 Molecular dynamics simulations of water wetting on SiC. (a) CA on 6H-SiC *vs.* charge Si/C-atom. More charge one atom possesses, the smaller the CA is. Inset: Side view snapshot of the water droplet on the C-face with C (−2.00*e*) and the Si-face with Si (+2.00*e*) of 6H-SiC. The white, red, yellow and cyan dots represent H, O, Si and C atoms, respectively. (b) CA on 4H-SiC *vs.* charge Si/C-atom. (c) Number density of molecules as a function of *Z*-distance from the surface for 6H-SiC with 2*e*. (d) Number density changes as a function of *Z*-distance from the surface for 4H-SiC with 2*e*.

the surface and water molecules. Therefore, it means that the interaction between the Si-face and water molecules is stronger than that between the C-face and water, causing a smaller contact angle. We also observe that the density of droplets becomes nearly zero at a height of 1.9 nm away from the Si-face and 3 nm away from the C-face, respectively, indicating that the Si-face has a stronger interaction than the C-face to make a smaller CA. For 4H-SiC in Fig. 6, positions of the first density peaks are 0.287 nm for both the Si-face and the C-face. But water droplets show a density value of 2.04 g cm^{-3} on the Si-face while 2.01 g cm^{-3} on the C-face. This means that the Si-face of 4H-SiC also has a stronger interaction than the C-face on water. From molecular dynamics simulations, we found that the density distribution of water droplets on the Si-face and the C-face strongly suggests that the interaction between the Si-face and water is stronger than that between the C-face and water. This is the reason why the CA on the Si-face is smaller than that on the corresponding C-faces.

The wetting difference of water on SiC can be developed as a new method to distinguish polar faces of polar single crystals.

This is a quick and facile method with the nontoxic water as a probe liquid. The distinguishing process brings no harm to tested samples and thus this method is nondestructive. Besides, the method is applicable to SiC samples with diameters of almost all lengths. We also investigate water wetting on other polar faces, such as those of zinc oxide single crystals. The CA of deionized water on the Zn-face (63°) is larger than that on the O-face (59°). This indicates that the wetting method can also be used to distinguish the Zn-face and the O-face of zinc oxide, representing a universally simple method for determining the polarity of crystal surfaces.

In the last few decades, several methods have been developed to distinguish polar faces, such as X-ray photoelectron spectroscopy,[32] transmission electron microscopy,[33] atomic force microscopy,[34] coaxial-impact-collision ion-scattering spectroscopy,[35] Auger electron spectroscopy[36] and chemical etching.[37] However, most of these methods are complex, expensive, time-consuming, and even destructive. Based on our results our method is more suitable and facile to distinguish the polar faces of large-sized SiC wafers with less cost for industrial applications.

Conclusion

Wetting on SiC single crystals with different stacking configurations is systematically investigated in this work. We find that the CA of deionized water on the C-face is larger than that on the Si-face for both conductive (N-doping) and semi-insulating (V-doping) SiC for both the 6H- and 4H-polytypes. There is almost no CA difference of tetrachloromethane on the C-face and the Si-face, indicating that surface roughness has no important influence on the CA. We also employ extensive molecular dynamics to simulate wetting of water on perfect SiC substrates and conclude that electrostatic interactions caused by charge transfer from the Si-atom to the C-atom in SiC induce such CA differences. These results will not only offer a reliable method to determine the polarity of SiC crystals quickly, simply, accurately and nondestructively, but also provide a promising method to determine the polarity of other polar crystals such as GaN, AlN and ZnO.

Acknowledgements

We acknowledge financial support from the National High Technology Research and Development Program (Grant No. 2014AA041402), MOST (Grant No. 2012CB921403), the National Natural Science Foundation of China (Grant No. 51272276, 51322211, 11474328, 11290164 and 11222431), and water project of CAS.

References

1 E. G. Shafrin and W. A. Zisman, *J. Phys. Chem.*, 1960, **64**(5), 519.
2 Y. M. Zheng, H. Bai, Z. B. Huang, X. L. Tian, F. Q. Nie, Y. Zhao, J. Zhai and L. Jiang, *Nature*, 2010, **463**, 640.
3 R. J. Good, *J. Adhes. Sci. Technol.*, 1992, **6**(12), 1269.
4 D. L. Tian, Y. L. Song and L. Jiang, *Chem. Soc. Rev.*, 2013, **42**(12), 5184.
5 N. Giovambattista, P. G. Debenedetti and P. J. Rossky, *J. Phys. Chem. B*, 2007, **111**, 9581.
6 C. Wang, H. J. Lu, Z. G. Wang, P. Xiu, B. Zhou, G. H. Zuo, R. Z. Wan, J. Hu and H. P. Fang, *Phys. Rev. Lett.*, 2009, **103**, 137801.
7 M. James, T. A. Darwish, S. Ciampi, S. O. Sylvester, Z. M. Zhang, A. Ng, J. J. Gooding and T. L. Hanley, *Soft Matter*, 2011, **7**, 5309.
8 C. Shih, Q. H. Wang, S. C. Lin, K.-C. Park, Z. Jin, M. S. Strano and D. Blankschtein, *Phys. Rev. Lett.*, 2012, **109**, 176101.
9 J. T. Lee, Y. Y. Zhao, S. Thieme, H. Kim, M. Oschatz, L. Borchardt, A. Magasinski, W. Cho, S. Kaskel and G. Yushin, *Adv. Mater.*, 2013, **25**, 4573.
10 Y. Zhang, K. Suenaga, C. Colliex and S. Iijima, *Science*, 1998, **281**, 973.
11 W. F. Koehl, B. B. Buckley, F. J. Heremans, G. Calusine and D. D. Awschalom, *Nature*, 2011, **479**, 84.
12 S. Castelletto, B. C. Johnson, V. Ivády, N. Stavrias, T. Umeda, A. Gali and T. Ohshima, *Nat. Mater.*, 2014, **13**, 151.
13 J. N. Stirman, F. A. Ponce, A. Pavlovska and I. S. T. Tsong, and David J. Smith, *Appl. Phys. Lett.*, 2000, **76**, 822.
14 C. Berger. Z.M. Song and X. B. Li, *et al.*, *J. Phys. Chem. B*, 2004, **18**, 19912.
15 C. Berger, Z. M. Song and X. B. Li, *et al.*, *Science*, 2006, **312**, 1191.
16 K. V. Emtsev, A. Bostwick and K. Horn, *et al.*, *Nat. Mater.*, 2009, **8**, 203.
17 J. Pezoldt, T. Kups, T. Stauden and B. Schröter, *Mater. Sci. Eng., B*, 2009, **165**, 28.
18 S. Fernández-Garrido, X. Kong, T. Gotschke, R. Calarco, L. Geelhaar, A. Trampert and O. Brandt, *Nano Lett.*, 2012, **12**, 6119.
19 M. Kusunoki, T. Suzuki, T. Hirayama, N. Shibata and K. Kaneko, *Appl. Phys. Lett.*, 2000, **77**, 531.
20 X. M. He, Z. M. Chen and L. Huang, *Mod. Phys. Lett. B*, 2015, **29**, 1550182.
21 H. J. C. Berendsen, J. R. Grigera and T. P. Straatsma, *J. Phys. Chem.*, 1987, **91**, 6269.
22 T. A. Darden, D. M. York and L. G. Pedersen, *J. Chem. Phys.*, 1993, **98**, 10089.
23 E. Lindahl, B. Hess and D. van der Spoel, *J. Mol. Model.*, 2001, **7**, 306.
24 E. Bekaroglu, M. Topsakal, S. Cahangirov and S. Ciraci, *Phys. Rev. B: Condens. Matter Mater. Phys.*, 2010, **81**, 075433.
25 T. Kato, T. Miura, K. Wada, E. Hozomi, H. Taniguchi, S. I. Nishizawa and K. Arai, *Mater. Sci. Forum*, 2007, **556**, 239.
26 D. Schulz, *et al.*, *Mater. Sci. Forum*, 2000, **338**(3), 87.
27 M. Bickermann, B. M. Epelbaum, D. Hofmann, T. L. Straubinger, R. Weingartner and A. Winnacker, *J. Cryst. Growth*, 2001, **233**, 211.
28 S. Nakashima, M. Higashihira and K. Maeda, *J. Am. Ceram. Soc.*, 2003, **86**, 823.
29 B. Song, H. Q. Bao, H. Li, M. Lei, T. H. Peng, J. K. Jian, J. Liu, W. Y. Wang, W. J. Wang and X. L. Chen, *J. Am. Chem. Soc.*, 2009, **131**, 1376.

30 Y. Liu, G. Wang, S. C. Wang, J. H. Yang, L. Chen, X. B. Qin, B. Song, B. Y. Wang and X. L. Chen, *Phys. Rev. Lett.*, 2011, **106**, 087205.
31 B. Groth and R. Haber, *Int. J. Appl. Ceram. Technol.*, 2015, **12**(4), 795.
32 M. H. Frommer, *J. Appl. Phys.*, 1987, **62**, 657.
33 F. Schuster, F. Furtmayr, R. Zamani, C. Magén, J. R. Morante, J. Arbiol, J. A. Garrido and M. Stutzmann, *Nano Lett.*, 2012, **12**, 2199.
34 A. Minj, A. Cros, N. Garro, J. Colchero, T. Auzelle and B. Daudin, *Nano Lett.*, 2015, **15**, 6770.
35 S.-K. Hong, T. Hanada, H. Makino, H.-J. Ko, Y. F. Chen and T. Yao, *J. Vac. Sci. Technol., B: Microelectron. Nanometer Struct.--Process., Meas., Phenom.*, 2001, **19**, 1429.
36 Y.-C. Lu, C. M. Stahle, J. Morimoto, R. H. Bube and R. S. Feigelson, *J. Appl. Phys.*, 1987, **61**, 925.
37 K. Nakagawa, K. Maeda and S. Takeuchi, *Appl. Phys. Lett.*, 1979, **34**, 574.